IFAC Workshop on Engine and Powertrain Control, Simulation and Modeling
Paris (France) November 30 - December 2, 2009

Model-Based Throttle Control using Static Compensators and IMC based PID-Design

Andreas Thomasson * **Lars Eriksson** *

* *Vehicular Systems, Dept. of Electrical Engineering Linköping University, SE-581 83 Linköping, Sweden, {andreast,larer}@isy.liu.se*

Abstract: In modern spark ignited engines the throttle is controlled by the electronic control unit (ECU) which gives the ECU direct control of the air flow and thereby the engine torque. This puts high demands on the speed and accuracy of the controller that positions the throttle plate. The throttle control problem is complicated by two strong nonlinear effects, friction and limp-home torque. This paper proposes the use of two, simultaneously active, static compensators to counter these effects and approximately linearize the system. A PID controller is designed for the linearized system, where IMC design is applied to design the PD controller and a gain scheduled I-part is added for robustness against model errors. A systematic procedure for generating compensator and controller parameters from open loop experiments is also developed. The controller performance is evaluated both in simulation, on a TC-benchmark problem, and experimentally. A robustness investigation pointed out that the limp-home position is an important parameter for the controller performance, this is emphasized by the deviations found in experiments. The proposed method for parameter identification achieves the desired accuracy.

Keywords: Limp home, friction compensation, internal model control, PID, automatic tuning.

1. INTRODUCTION

An electronic throttle is a DC-servo that controls the throttle plate in modern spark ignited (SI) engines. The position of the throttle plate controls the air-flow to the engine and hence the engine torque. As a consequence this servo is a very important component in a vehicle since it affects the vehicle driveability.

Throttle control design is challenging due to two non-linearities, friction and limp-home torque, which effects the throttle plate motion. Strategies for overcoming these difficulties have been addressed in several papers. A model based friction compensator was presented in Eriksson and Nielsen (2000) and a nonlinear control strategy with both friction and limp-home compensation is proposed in Deur et al. (2006). Another approach was made in Vašak et al. (2006), where a control law based on the solution of an optimal control problem was demonstrated.

This paper makes use of friction and limp-home compensators that are static functions of the measured throttle position and reference value, to remove most non-linearities. This is a combination and simplification of ideas presented in Eriksson and Nielsen (2000) and Deur et al. (2006). The compensated system is controlled by a PID-controller which is tuned with the IMC technique to give a first order behavior to the linearized system. Further a systematic procedure for tuning the controller is developed which is similar to that suggested in Pavković et al. (2006).

⋆ This research was supported by the VINNOVA Industry Excellence Center LINK-SIC and by the Strategic Research Center MOVIII, funded by the Swedish Foundation for Strategic Research.

In the next section a simplified model for an electronic throttle is presented with the aim of controller design. Section 3 describes the controller structure and its three main parts: friction compensator, limp-home compensator and PID-controller. In section 4, a procedure for identifying the controller parameters are discussed. The controller performance and robustness to parameter variations is verified in simulation on the benchmark model in section 5 and experimentally on a throttle in section 6.

2. CONTROL ORIENTED THROTTLE MODEL

In this section the throttle model, that is used to design the controller in section 3, is presented. Figure 1 show a sketch of the throttle system. The control signal is transformed to a PWM signal by the chopper that is connected to the DC motor. The motor torque is transferred to the throttle plate axle through a gearbox (not shown in figure). The return spring exercises a torque on the throttle plate that pulls it toward the limp-home position.

The torque acting on the throttle plate is split into four main parts. The driving torque from the DC motor, T_u,

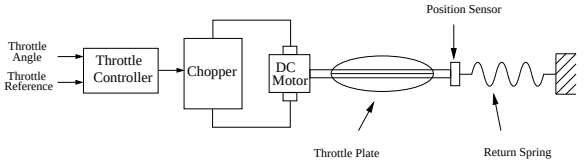

Fig. 1. A schematic of the electronic throttle and controller. Main parts are the controller (which is part of the ECU), chopper, DC motor, throttle plate, return spring and position sensor.

the spring torque, T_s, the static friction torque, T_{fs}, the dynamic friction torque, T_{fv} and the back electromotive force, T_e. After modeling the separate torque contributions, the equations of motion for the throttle plate are given by Newtons second law.

$$\begin{cases} \dot{\theta} &= \omega \\ J\dot{\omega} &= T_u - T_s - T_{fs} - T_{fv} - T_e \end{cases} \tag{1}$$

Both the friction and limp-home nonlinearity can be seen from the process static curve which is illustrated in figure 2. This curve can be estimated by performing a slow ramp in the control signal while measuring the response in throttle position. The influence of friction is clearly seen from the difference in the ramp up and down in control signal.

The static friction T_{fs} is modeled using a classical Coulomb friction model, Olsson et al. (1998), seen in (2). The friction torque T_{fs} is equal to the applied torque T when $\omega = 0$ and the applied torque is less than the Coulomb friction, T_c. Otherwise the friction torque is equal to T_c in the opposite direction of motion.

$$T_{fs}(T,\omega) = \begin{cases} T & \text{if } \omega = 0 \text{ and } |T| < T_c \\ T_c sgn(\omega) & \text{otherwise} \end{cases} \tag{2}$$

The limp-home nonlinearity comes from the springs that pulls the throttle plate toward the limp-home position. The spring force is piecewise linear but the spring constant differs greatly, depending on whether the throttle plate is below, inside, or above the limp-home position. The spring force is therefore described as the piecewise linear function in the equation below and is illustrated in figure 3.

$$T_s(\theta) = \begin{cases} m_{lh}^+ + k^+(\theta - \theta_{lh}^+) & \text{if } \theta > \theta_{lh}^+ \\ m_{lh}^+(\theta - \theta_{lh})/(\theta_{lh}^+ - \theta_{lh}) & \text{if } \theta_{lh} < \theta \le \theta_{lh}^+ \\ m_{lh}^-(\theta_{lh} - \theta)/(\theta_{lh} - \theta_{lh}^-) & \text{if } \theta_{lh}^- < \theta \le \theta_{lh} \\ m_{lh}^- - k^-(\theta_{lh}^- - \theta) & \text{if } \theta \le \theta_{lh}^- \end{cases} \tag{3}$$

The models for viscous friction and electromotive force are both linear functions in angular velocity acting in the opposite direction of motion. They are lumped into a single torque model

$$T_{fv} + T_e = -K_{fv}\omega \tag{4}$$

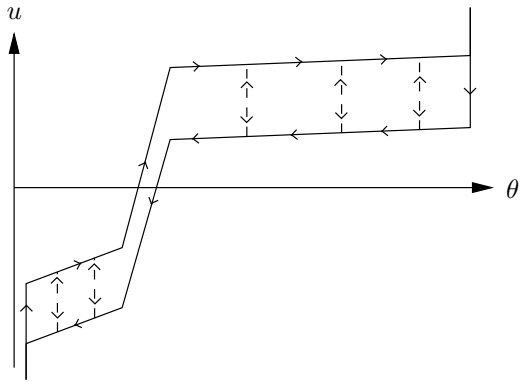

Fig. 2. Sketch of the static nonlinearities for the electronic throttle. arrows indicate the direction of movement. The influence of friction and the nonlinear spring torque is clearly seen. Compare with the real measured curve shown in figure 7.

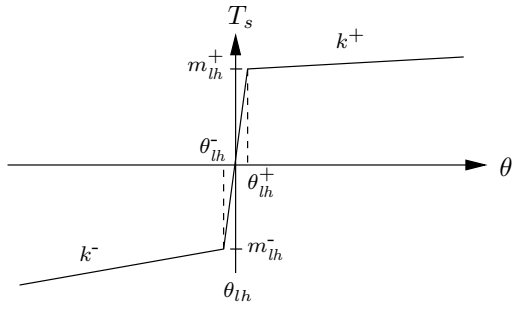

Fig. 3. A graphical representation of the model for the spring torque T_s which is a piecewise linear function of the throttle position.

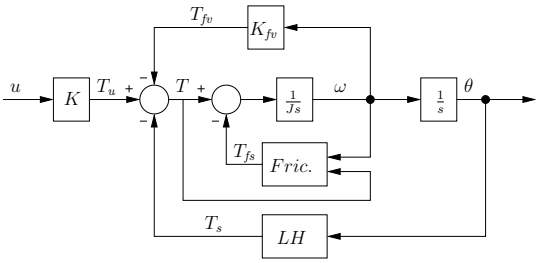

Fig. 4. A block diagram, showing the process model.

Combining (1), (2), (3), and (4), gives the equation for the throttle plate angular velocity

$$J\frac{d\omega}{dt} = -K_{fv}\omega - T_s(\theta) - T_{fs}(T,\omega) + Ku \tag{5}$$

The complete model is also shown as a block diagram in figure 4.

3. CONTROLLER STRUCTURE

To linearize the system in (5) a nonlinear compensator block that modifies the control signal u is proposed. The main idea is to choose the control signal as

$$u = \frac{T_s(\theta)}{K} + \frac{T_{fs}(T,\omega)}{K} + \tilde{u} \tag{6}$$

which would be an exact linearization of (5). This is not possible due to several reasons, but can be done approximately by the compensator blocks described in the two following sections. The linearized system is then controlled by a slightly modified PID-controller described in section 3.4.

3.1 Limp-home compensator

The limp-home compensator uses (3) with the commanded throttle reference, θ_{ref}, as the input instead of the actual (or measured) throttle angle, θ, see figure 3. Effectively this is a feedforward with the inverse static gain of the system as output.

3.2 Friction compensator

Based on (2) the compensator would be an ideal relay that switches sign around $\omega = 0$. This creates a problem with estimating the speed and direction of the throttle plate motion based on the position measurements. It is also not beneficial if the throttle plate currently is moving away

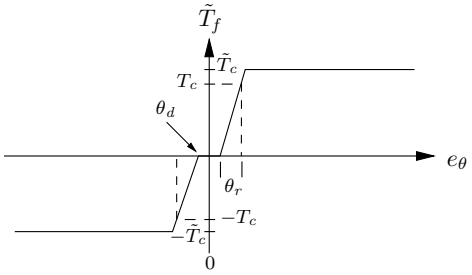

Fig. 5. The friction compensation is implemented as a static function of the tracking error. A small dead zone and a smooth transition is used around $e_\theta = 0$ to make the compensation less sensitive and avoid oscillations close to the reference value.

from the reference value and the friction compensator add to that motion. Instead the friction compensator is based on the present tracking error and compensation is made in the direction the controller wants to move the throttle plate to. An ideal relay function would be very sensitive to noise around $e_\theta = 0$ and would also cause undesirable oscillations around the reference value. This problem is solved with a small dead zone around the reference value and a smooth transition when e_θ increases. The dead zone radius is denoted θ_d and the width of the transition θ_r, see figure 5 and equation 7.

$$\tilde{T}_f(e_\theta) = \begin{cases} 0 & \text{if } |e_\theta| \leq \theta_d \\ \tilde{T}_c \dfrac{\theta - \theta_d}{\theta_r} sgn(e_\theta) & \text{if } \theta_d < |e_\theta| \leq \theta_r + \theta_d \\ \tilde{T}_c sgn(e_\theta) & \text{if } |e_\theta| > \theta_r + \theta_d \end{cases} \quad (7)$$

When the throttle plate is close to the reference value, the large part of the control signal comes from the friction compensator block. If the Coulomb friction were underestimated the rise time could get unnecessary long after small changes in reference position. To make sure that the friction compensator overcomes the Coulomb friction the maximum amplitude of the compensator block is increased to $\tilde{T}_c = T_c * k$, where k is slightly larger than one. Also the Coulomb friction is different above and below the limp-home position and its values are distinguished by T_c^+ and T_c^- respectively.

The limp-home and friction compensators are used to modify the control signal according to (8) where $\tilde{u}$ is the output from the PID-controller described in the next section.

$$u = \frac{T_s(\theta_{ref})}{K} + \frac{\tilde{T}_f(e_\theta)}{K} + \tilde{u} \quad (8)$$

3.3 The linear system

With the control signal selected according to (8) and the compensators in section 3.1 and 3.2, the system is approximately linear and given by the equation below.

$$J\frac{d\omega}{dt} = -K_{fv}\omega + K\tilde{u} \quad (9)$$

To simplify notation the equation is normalized by K_{fv} and the parameters $T_0 = \frac{J}{K_{fv}}$ and $K_0 = \frac{K}{K_{fv}}$ are introduced. The resulting differential equation is

$$T_0\frac{d\omega}{dt} = -\omega + K_0\tilde{u} \quad (10)$$

And the resulting transfer function from $\tilde{u}$ to θ is

$$\theta(s) = \frac{K_0}{s(T_0 s + 1)}\tilde{u} \quad (11)$$

The throttle position is normalized to $[0, 100]$ and the control signal is normalized to $[-100, 100]$.

3.4 IMC-based PID design

To avoid hitting the mechanical stops at the end positions, the response to a reference step should have no overshoot. The IMC-framework for controller design, Garcia and Morari (1982); Rivera et al. (1986), is used to give the closed loop system a first order behavior according to

$$G_c = \frac{1}{\lambda s + 1} \quad (12)$$

which gives the following PD-controller

$$F_{PD}(s) = K_p + K_d s \quad (13)$$

with the parameters $K_p = \frac{1}{K_0\lambda}$ and $K_d = \frac{T_0}{K_0\lambda}$. The tuning parameter λ is the desired time constant for the closed loop system.

This rise time will of course only be achieved when the control signal does not saturate. Unfortunately this will be the case for larger reference steps if the product $K_0 \cdot \lambda$ is smaller than about one. How this and other nonlinear effects are compensated for will be discussed in section 4.

Filter on D-part To reduce the effect of measurement noise the derivative part of the controller is filtered with a first order low pass filter. The filter equation is

$$Y(z) = \frac{1 - \gamma}{1 - \gamma z^{-1}}U(z) \quad (14)$$

3.5 A modified I-part

A prerequisite to get the closed loop system behavior in (12) is that the model is correct. Even with a correct model the approximations in the linearization or input disturbances etc. could result in a stationary tracking error. To compensate for this a modified I-part is added to the controller. The integrator gain K_i is gain scheduled. It is zero when the error is large and increases with decreasing error. This will prevent integrator wind-up during large transients and help to quickly overcome model errors for small changes in reference. The error input to the integrator is also slightly modified. When the tracking error is smaller than half the resolution of the position measurement, the error is set to zero. Two reset conditions are also used. When the throttle reference makes a step larger than 0.5% or when the control signal saturates, the integrator is set to zero.

A block diagram of the implemented controller structure is shown in figure 6.

4. IDENTIFICATION AND CONTROLLER TUNING

In order to be able to automate the controller parametrization, two experiments were developed. The experiments are designed to identify the model parameters that directly give the controller parameters in the model-based controller. Both compensator blocks are identified from a ramp response in control signal, described in section 4.1, while the PID-parameters are determined using a step response, described in section 4.2.

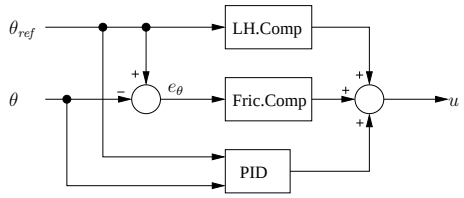

Fig. 6. A block diagram of the controller structure. The control signal u is the sum of the outputs from the compensator blocks and the PID-controller.

4.1 The static compensators - ramp response

Both the friction and limp-home nonlinearities are estimated from the process static curve which was illustrated in figure 2. This characteristic can be measured by doing a slow ramp response up and down in the throttle control signal, see figure 7. The proposed method for calculating the limp-home and friction compensators uses the points A_1-A_4 and B_1-B_4 marked in the figure. The equations for calculating the parameters below the limp-home position are given in (15), the others are determined in an equivalent manner.

$$\theta_{lh} = \frac{\theta(A_2) + \theta(A_3) + \theta(B_2) + \theta(B_2)}{4} \tag{15a}$$

$$\bar{\theta_{lh}} = \frac{\theta(A_2) + \theta(B_2)}{2} \tag{15b}$$

$$\bar{m_{lh}} = \frac{u(A_2) + u(B_2)}{2} \tag{15c}$$

$$\bar{k} = \frac{u(A_2) - u(A_1)}{\theta(A_2) - \theta(A_1)} \tag{15d}$$

The dead zone and transition in the friction compensator should be made small to get precise control for small changes in reference. Making them too small however can cause oscillations around the reference value. In simulation and experimentally $\theta_d \approx 0.1\%$ and $\theta_r \approx 0.5\%$ have proved to work satisfactory.

4.2 P and D parameters - step response

After the static curve has been determined a step response is made to identify the linear process dynamics. Starting

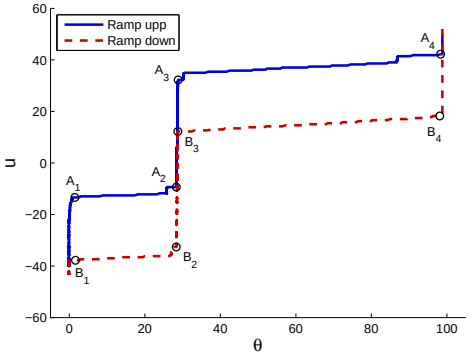

Fig. 7. Measured ramp response in throttle position, the solid line (blue) is when u is increasing and the dashed line (red) when u is decreasing. The marked points A1-A4 and B1-B4 are used in the calibration procedure when calculating the friction and limp-home compensators.

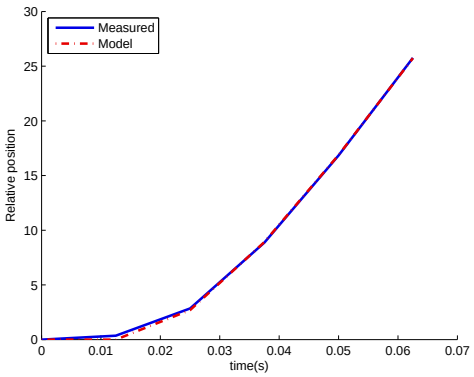

Fig. 8. A measured step response together with simulation of the adapted process model. The initial position before the step has been set to zero.

with the throttle in the limp-home position the control signal is ramped up until the position is slightly larger then θ_{lh}^{+}. Then a step in control signal is applied and the position response is measured. The parameters in (11) are fitted with the least mean squares method to the step response. A measured step response and the adapted model can be seen in figure 8.

The parameters K_p and K_i are given by (16) and follow directly from the analysis in section 3.4. The difference is in the derivative part that has been increased by a factor of three. Both the simulation and the experimental work showed that the ideal choice $K_d = \frac{T_0}{K_0\lambda}$ proved to be too small, resulting in position overshoot and thus the derivative part where increased.

$$K_p = \frac{1}{K_0\lambda} \tag{16a}$$

$$K_d = \frac{3T_0}{K_0\lambda} \tag{16b}$$

How to choose λ The tuning parameter λ gives the rise time of the closed loop system. This can be translated into an arbitrary demand of the form "within X % in t seconds" by considering the step response of the system in (12) to a unit step in reference.

$$y(t) = 1 - e^{-t/\lambda} \tag{17}$$

Setting $y(t) = X$ and solving for λ gives:

$$\lambda = \frac{-X}{ln(t)} \tag{18}$$

As was previously mentioned, this is only true when the control signal does not saturate. The increase in rise time due to signal saturation during large reference steps could be somewhat compensated for by decreasing λ. This will saturate the control signal for a longer period of time than with the original setting, thereby making up for lost time at the end of the step response. This will be limited by the shortest possible rise time achieved with a saturated signal during the whole step.

The filter coefficient In the controller the filter coefficient $\gamma = 0.7$ is used for the filter on the D-part, which for a sampling time of 1 ms gives the filter a settling time (within 5% of end value) of less then 10 ms.

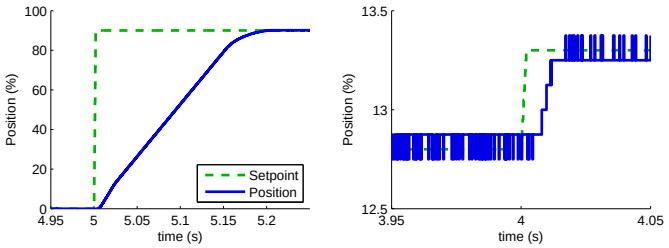

Fig. 9. Two different sized step responses in θ_{ref} (part of signals A1.1 and A3.2) simulated on the benchmark model. Settling time for the large step are less than 170 ms and the overshoot smaller than 0.25%.

4.3 The I-part

The I-part of the controller is gain scheduled, using the tracking error to determine the integrator gain K_i. When $|e_\theta|$ is larger than 10%, the integrator is turned off, $K_i = 0$. As $|e_\theta|$ decreases from 10% to 1%, K_i increases linearly from 0 to 10. From that point K_i increases to 100 at $|e_\theta| = 0.5\%$ and remains constant when $|e_\theta| \leq 0.5\%$.

5. SIMULATION RESULTS ON TC BENCHMARK MODEL

The procedure described in section 4 has been performed on the benchmark model provided by E-COSM'09, Zito et al. (2009), and resulted in the controller parameters in table 1.

Table 1. Controller parameters identified with the two experiments on the benchmark model.

K_p	8.53	θ_{lh}	11.1	m_{lh}^-	-10.9
K_d	0.051	θ_{lh}^+	11.3	k^+	0.051
T_c^+	8.76	θ_{lh}^-	10.9	k^-	0.065
T_c^-	6.83	m_{lh}^+	9.03		

The controller performance is evaluated using the different reference signals provided by the benchmark model. These include series of steps, ramps, and more arbitrary signals. Two different sized step responses are shown in figure 9. For the large step the controller saturates the control signal until almost within 10% of the reference which indicates that the step response could not get much faster and the overshoot is less then 0.25%. For the small step the throttle position is within the quantization error from the reference value in less then 12 ms. A ramp response (part of signal A2.2) and corresponding tracking error are shown in figure 10. A small stick slip motion of the throttle is evident in the figure but the error does not exceed 0.3% during the ramp, which is small. All these results must be considered good and meet the demands on an automotive throttle controller.

The integral square error for all provided test signals in the throttle benchmark with the presented controller are given in table 2. The initial throttle position was set equal to the initial reference value for each test.

5.1 Robustness investigation

One critical parameter in the controller is the accuracy of the limp-home position. Due to the step-like characteristic

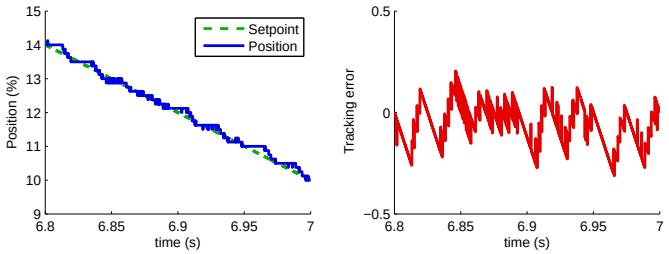

Fig. 10. Simulated ramp response (the end of signal A2.2) and corresponding tracking error while passing through the limp-home position, which is around 11.1%. Peak tracking error is approximately 0.3%.

Table 2. Performance measures for the tests defined in the TC benchmark.

A1.1	A1.2	A1.3	A2.1	A2.2	A3.1	A3.2
837	152	21.2	0.123	0.094	1036	508

of the static curve, incorrect information in the controller could lead to degraded controller performance around this position. Another important parameter is the amplitude of the friction compensator. During operation with only small changes in reference around a nominal value, a large part of the control signal comes from the friction compensator block. A bad estimate of the coulomb friction could have large effect on the controller performance for small reference changes. To investigate the influence of incorrect limp-home and friction compensation a series of test have been made.

Error in limp-home position Figures 11, 12, 13 and 14 show comparisons between the nominal controller and controllers that have an error in the limp-home compensator. In the figures to the left the limp-home compensator has the limp-home position at 11% which is the same as the actual position. In the figures to the right the limp-home compensator has the limp-home position at 11% while the actual limp-home position is at 13%. In figure 11 the controller starts to compensate for the limp-home position when the reference step to 11% is made, resulting in a small overshoot and oscillations. In figure 12 a ramp response through the limp-home position is compared. For the controller with incorrect limp-home position the throttle position deviates slightly from the reference ($\leq 1.5\%$) both

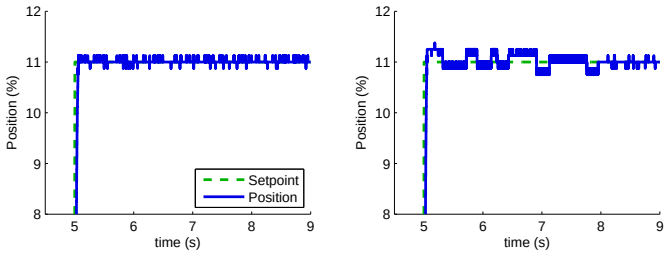

Fig. 11. *Left:* The controller has correct information of the limp-home position. *Right:* The controller has a 2% error in limp-home position. The limp-home compensator starts to compensate below the limp-home position, resulting in an overshoot and small oscillations.

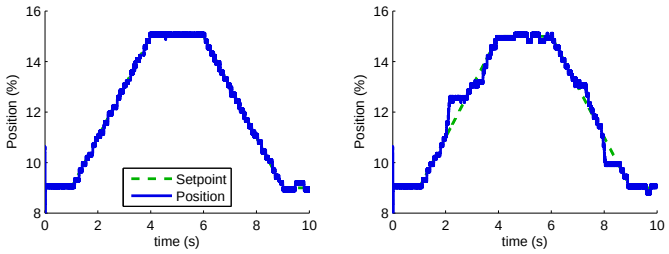

Fig. 12. *Left:* The controller has correct information of the limp-home position. *Right:* The controller has a 2% error in limp-home position. When the reference passes the actual limp-home position (13%) and where the controller believes the limp-home position is (11%), the controller rises to about 1% before the integrator compensates the error in the limp-home compensator.

where the controller believes the limp-home position is, and at the actual limp-home position.

Figure 13 shows step responses around the limp-home position with both the correct and the incorrect controller. The incorrect controller compensates for the limp-home position before it has been reached, leading to relatively large overshoot compared to the step size. In figure 14 the behavior when doing steps into the limp-home position is shown. With an error in the controller, the position over- or undershoots of about 0.5%.

An error in the limp-home compensator has a large effect on the controller performance when operating between the limp-home position in the controller and the actual limp-home position. The largest impact is seen in figure 13 and could lead to oscillations in the engine air flow that would result in oscillations in torque. This behavior would be unacceptable in a production vehicle and thus this controller requires good precision in the parameter θ_{lh} in the limp-home compensator, within a few tenths of a percent. The significance of this is further strengthened by experiments with real throttles, that have shown that there can be significant differences in the limp-home position between individual throttles. In particular a deviation larger than 2 % has been found between an engine in an engine test cell and an identical engine in a vehicle. However the desired accuracy is achieved with the presented tuning method. Effects like aging of the throttle and position sensor or production deviations could be handled by running a calibration at each start up. If a full calibration is not possible, it is suggested that the system performs a simpler diagnosis and calibration by measuring the throttle position with zero control signal which gives an accurate enough measurement of the limp-home position.

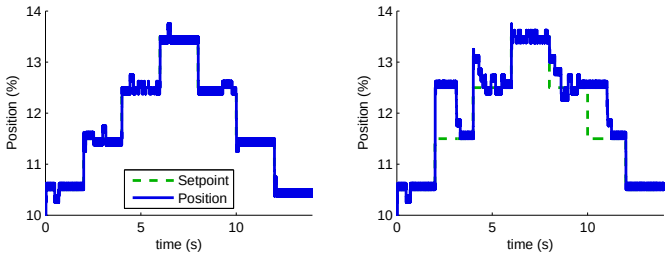

Fig. 13. *Left:* The controller has correct information of the limp-home position. *Right:* The controller has a 2% error in limp-home position. The worst case scenario with limp-home position error. Small steps between the expected and actual limp-home position will cause over and undershoots of about 1%

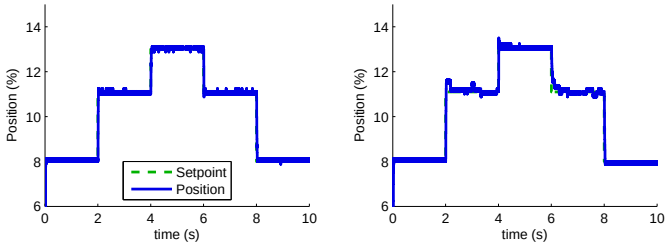

Fig. 14. *Left:* The controller has correct information of the limp-home position. *Right:* The controller has a 2% error in limp-home position. The effect of the error in the controller is a small over and undershoot when doing steps to the limp-home position.

Error in friction compensator Figure 15 and 16 compare the controller performance with correct friction estimation and where the friction has been underestimated, respectively overestimated, of 30%. In both cases, small oscillations around the reference value are introduced and an overestimated friction tends to increase the position overshoot. These oscillations are however fairly small and do not have a large effect on vehicle driveability. The controller does not seem to be very sensitive to friction compensator errors of this magnitude.

6. EXPERIMENTAL RESULTS

The control design and tuning procedure have also been applied to the throttle in an engine test cell. The controller was evaluated using similar input signals as the benchmark

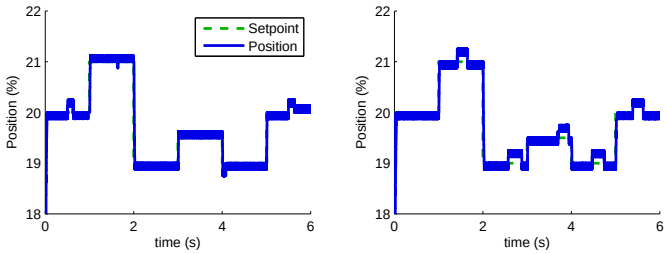

Fig. 15. *Left:* The controller friction compensation is correct. *Right:* The friction compensator underestimates the friction of 30%.

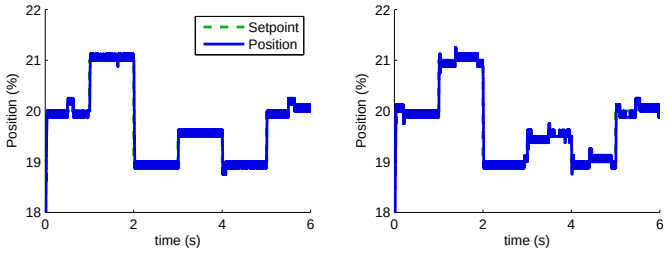

Fig. 16. *Left:* The controller friction compensation is correct. *Right:* The friction compensator overestimates the friction of 30%.

model, however the ramp response became a sequence of small steps due to a low sampling rate of the manual input signal used as reference. A large and a small step response are shown in figure 17 and the "ramp" and corresponding tracking error are shown in figure 18. The step response is slightly slower in the experimental tests but also has less overshoot. Hence the response time can be decreased with a smaller λ but at the expense of a larger overshoot, which shows that the nominal design gives a controller with the desired behavior. This thus shows that the controller achieves satisfactory results also in experiments. These experimental results further strengthens the conclusion that the developed throttle controller gives good performance and the tuning method is straightforward to apply. Furthermore the controller performance is easy to tune with the aid of the IMC tuning parameter γ.

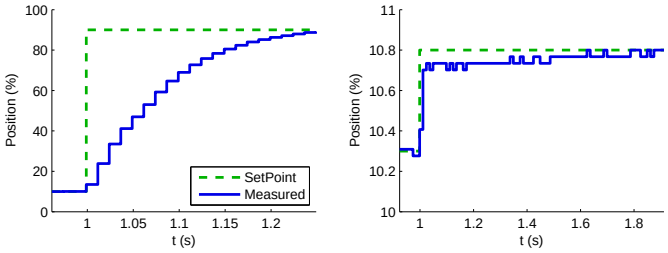

Fig. 17. Two experimental step responses of different magnitude of different magnitude. The settling time for the large step is less than 200 ms and the overshoot is smaller than 0.1%.

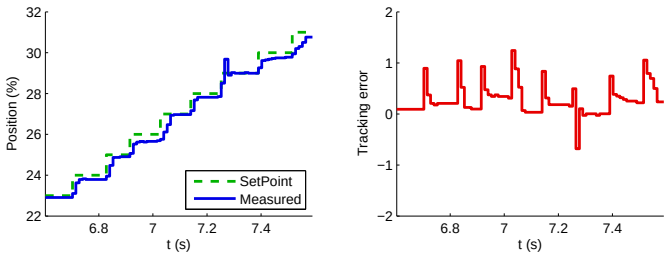

Fig. 18. An experimental ramp response and corresponding tracking error which is slightly larger than on the simulation model. The peaks in the error signal is mainly because the more step-like reference signal.

7. CONCLUSIONS

A throttle control strategy based on two static compensators and a PID controller has been presented. A tuning method for the parameters in both the compensators and the PID controller has also been developed. The relatively simple controller has been shown to give good performance both in simulation and in experiments. A robustness investigation has also been performed with respect to the friction and limp-home nonlinearities. An important result is that the controller is sensitive to how well the limp-home position is known. The accuracy of this controller parameter must be within a few tenths of a percent of the actual position in order to give a satisfactory control behavior in the neighborhood of the limp-home position. Experimental data have shown that deviations of a few percent can occur which thus can pose a problem if this is not accounted for. The proposed design method with the proposed calibration procedure achieves a sufficiently accurate calibration. However, a simpler strategy for diagnosing and amending possible problems is to calibrate the limp-home position at each start up by registering and storing the throttle position with zero control signal.

REFERENCES

Deur, J., Pavković, D., Perić, N., Jansz, M., and Hrovat, D. (2006). An electronic throttle control strategy including compensation of friction and limp-home effects. *IEEE Transactions on Industry Applications*, 40, 821–834.

Eriksson, L. and Nielsen, L. (2000). Non-linear model-based throttle control. In *Electronic Engine Controls*, volume SP-1500, 47–51. SAE 2000 World Congress, March 2000, Detroit, MI, USA.

Garcia, C.E. and Morari, M. (1982). Internal model control. 1. a unifying review and some new results. *Ind. Eng. Chem. Process. Des. Dev.*, 21, 308–323.

Olsson, H., Åström, K., de Wit, C.C., Gäfvert, M., and Lischinsky, P. (1998). Friction models and friction compensation. *European Journal of Control*, 4(3), 176–195.

Pavkvić, D., Deur, J., Jansz, M., and Perić, N. (2006). Adaptive control of automotive electronic throttle. *Control Enginering Practice*, 14, 121–136.

Rivera, D.E., Morari, M., and Skogestad, S. (1986). Internal model control. 4. pid controller design. *Ind. Eng. Chem. Process. Des. Dev.*, 25, 252–265.

Vašak, M., Baotić, M., Morari, M., Petrović, I., and Perić, N. (2006). Constrained optimal control of an electronic throttle. *International Journal of Control*, 79, 465–478.

Zito, G., Tona, P., and Lassami, P. (2009). "The Throttle Control Benchmark". In *Proceedings of E-COSM'09*. IFAC Workshop on Engine and Powertrain Control, Simulation and Modeling, IFP Rueil-Malmaison, France, 2009.